QBER: Quantum-based Entropic Representations for Un-attributed Graphs

Lixin Cui[a], Ming Li[b,d,*], Lu Bai[c,a,**], Yue Wang[a], Jing Li[a], Yanchao Wang[a], Zhao Li[e,f], Yunwen Chen[g], Edwin R. Hancock[h]

[a]*Central University of Finance and Economics, Beijing, China.*
[b]*Key Laboratory of Intelligent Education Technology and Application of Zhejiang Province,: Zhejiang Normal University, Jinhua, China.*
[c]*School of Artificial Intelligence, Beijing Normal University, Beijing, China.*
[d]*Key Laboratory of Scientific and Engineering Computing (Ministry of Education), Shanghai Jiao Tong University, Shanghai, China.*
[e]*Hangzhou Link2Do Technology Ltd, Zhejiang, China.*
[f]*Alibaba-ZJU Joint Research Institute of Frontier Technologies, Zhejiang, China.*
[g]*DataGrand Inc, Shanghai, China.*
[h]*Department of Computer Science, University of York, York, UK.*

Abstract

In this paper, we propose a novel framework of computing the Quantum-based Entropic Representations (QBER) for un-attributed graphs, through the Continuous-time Quantum Walk (CTQW). To achieve this, we commence by transforming each original graph into a family of k-level neighborhood graphs, where each k-level neighborhood graph encapsulates the connected information between each vertex and its k-hop neighbor vertices, providing a fine representation to reflect the multi-level topological information for the original global graph structure. To further capture the complicated structural characteristics of the original graph through its neighborhood graphs, we propose to characterize the structure of each neighborhood graph with the Average Mixing Matrix (AMM) of the CTQW, that encapsulates the time-averaged behavior of the CTQW evolved on the neighborhood graph. More specifically, we show how the AMM matrix allows us to compute a Quantum Shannon Entropy for each vertex, and

---

*Corresponding Author
**Corresponding Author
Email addresses: cuilixin@cufe.edu.cn (Lixin Cui), mingli@zjnu.edu.cn (Ming Li), bailu@bnu.edu.cn; bailucs@cufe.edu.cn (Lu Bai), wangyuecs@cufe.edu.cn (Yue Wang), lijing2017@cufe.edu.cn (Jing Li), wangyanchao@cufe.edu.cn (Yanchao Wang), lizhao.lz@alibaba-inc.com (Zhao Li), chenyunwen@datagrand.com (Yunwen Chen), edwin.hancock@york.ac.uk (Edwin R. Hancock)

thus compute an entropic signature for each neighborhood graph by measuring the averaged value or the Jensen-Shannon Divergence between the entropies of its vertices. For each original graph, the resulting QBER is defined by gauging how the entropic signat ures vary on its k-level neighborhood graphs with increasing k, reflecting the multi-dimensional entropy-based structure information of the original graph. Experiments on standard graph datasets demonstrate the effectiveness of the proposed QBER approach in terms of the classification accuracies. The proposed approach can significantly outperform state-of-the-art entropic complexity measuring methods, graph kernel methods, as well as graph deep learning methods.

1. Introduction

In pattern recognition, graph-based representations can well describe pairwise relationships between components for structure data analysis, e.g., 3D shapes [1, 2], social networks [3, 4], protein networks [5, 6], etc. The main challenge arising in graph data analysis is how to represent a graph structure in a manner that can preserve the structural characteristics for graph classification. To achieve this, one popular way is to develop novel methods that can compute the numeric characteristics from the discrete graph structure [7, 8]. Specifically, these approaches are the so-called graph embedding methods that can embed or represent the graph structure as a vectorial representation, so that standard pattern recognition algorithms can be directly employed for graph classification or clustering [9, 10]. This paper aims to propose a novel framework of computing quantum entropy-based numeric representations, for the purpose of graph classification. Our approach can reflect rich complicated intrinsic graph characteristics through quantum walks [11], explaining the effectiveness.

1.1. Related Works

In the literature, there have been many novel approaches that can well embed graph structures into vectorial representations for graph-based data analysis. For instance,

Wilson et al. [12] have developed a spectrum-based approach to compute the vectorial graph representations based on algebraic graph theory. Specifically, they employ the spectral decomposition of the graph Laplacian, and compute the symmetric polynomial invariants of graphs associated with the eigenvectors. Bunke et al. [13] have transformed graphs into vectorial representations through either the vertex or edge attributed statistics. Ren et al. [14] have computed vectorial representations of graphs by counting the numbers of cycles with different lengths, through the Ihara zeta function. Kondor and Borgwardt [15] have computed vectorial representations of graphs through graph skew spectrum features. He et al. [16] have developed a Adversarial representation mechanism GAN (ArmGAN) model to learn vectorial representations of graphs, based on the adversarial learning scheme. One common drawback arising in these state-of-the-art methods is that they tend to represent graph structures in a low dimensional vector space, and may thus neglect intrinsic structural information residing on the topological structures of graphs.

To address the above problem, in recent years the quantification of the structural complexity of graphs has attracted important attentions, due to the fact that the graph complexity measures can significantly reflect the intrinsic structural information of graphs and have been proven effective tools for graph data analysis. Generally speaking, there are two main strategies to compute graph complexities, i.e., (a) the deterministic complexity measures, as well as (b) the probabilistic complexity measures. Approaches based on the fiRst strategy depend on the encoding [17], subgraph counting [18, 19, 20] and structure generating [21] of graph structures. On the other hand, approaches based on the second strategy mainly depend on measuring the graph entropy associated with a probability distribution of each graph. Viewed theoretically, the entropy-based complexity measures developed in recent years are mainly based on the statistical graph features, e.g., the vertex degree, the edge density, the Laplacian spectrum, etc. Thus, these entropy-based complexity measures can capture more correlation information between local vertices based on the statistical graph features, and usually have more effective performance than the deterministic complexity measures. In this work, we focus more on employing the graph entropy as a means of defining novel graph embedding methods, reflecting the complicated intrinsic structure infor-

mation of graphs.

Unfortunately, computing the graph entropy in a straightforward way is not a simple problem. In previous works, Körner [22] has proposed an entropy-based complexity measure by posing the structural characterization as an optimization task. Specifically, the complexity measure of a graph is defined by computing the minimal cross entropy between an associate probability distribution of the vertices and the vertex packing polytype of the graph. Dehmer et al. [23, 24, 20] have proposed a family of information theoretic graph entropy measures based on information functionals, that quantify the information content of the topological structure of a given graph. Since the required information functionals can be constructed through the local subgraph of the given graphs and avoid the combinatorial computations over different vertex partitions, these entropy measures can be efficiently computed in a polynomial time.

Another interesting idea of computing the graph entropy refers to the concept of quantum mechanics [25], and a number of quantum-based graph entropy measures have been developed. For instance, Anand et al. [26] and Passerini et al. [27] have proposed a family of von Neumann entropies based on the quantum state of a graph [25]. Specifically, they map the quantum state into the discrete graph Laplacian [28], that can be seen as a density matrix if it is scaled by the inverse of the graph volume. The resulting von Neumann entropy of a graph can be computed based on the discrete graph Laplacian. Furthermore, they show that the quantum-based von Neumann entropy is related to the classical Shannon entropy if there is the degree heterogeneity. Unfortunately, computing the von Neumann entropies depends on the decomposition of the normalized Laplacian spectrum, that requires time complexity of cubic vertex numbers. To further improve the computational efficiency for the von Nenmann entropy, Han et al. [29] have exhibited how the computation can be further improved to quadratic vertex numbers by adopting a quadratic approximation of the Shannon entropy associated with the eigenvalues of the Laplacian matrix. This reveals that the von Neumann entropy can be calculated based on the expressions of the permutation invariant matrix trace, leading to a simple expression for the approximate von Neumann entropy in terms of the vertex degrees. To develop this work one step further, Ye et al. [30] have generalized the approximate von Neumann entropy from undirected graphs into direct-

4

ed graphs. To achieve this, they first employ Chung's [31] definition of the normalized Laplacian for directed graphs. Based on this definition, the normalized Laplacian matrix of a directed graph is Hermitian, and thus the interpretation stated by Passerini et al. [26] still maintains for directed graphs. This indicates that the von Neumann entropy of the normalized Laplacian matrix can be essentially the Shannon entropy associated with its eigenvalues, providing an theoretical expression of the von Neumann entropy for directed graphs associated with the in-degree and out-degree residing on the vertices of the directed graphs.

To further reflect interior structural information for graphs, recently a number of thermodynamic entropy measures have been developed. For instance, Wang et al. [32] have developed an entropic graph representation method based on the thermodynamic edge entropy decomposition associated with the spin statistics. Specifically, they investigate three spin-dependent statistical models to determine the thermodynamic entropy of a network, including (a) the classical spinless Maxwell-Boltzmann distribution, and two models based on quantum mechanical spin-statistics, namely (b) the Bose-Einstein model for particles with integer spin, and (c) the Fermi-Dirac model for particles with half-integer spin. Zhang et al. [33] have developed a graph motif entropy measure based on motifs, i.e., the subgraphs recurring most frequently over different graphs. Specifically, they employ the motifs as the graph primitives based on the concept of cluster expansion from statistical physics. By mapping the network motifs to clusters in the gas model, they derive the partition function for a graph structure to compute global thermodynamic quantities, e.g., the energy and entropy. Both entropy-based methods can capture intrinsic complicated structural information through the thermodynamic characteristics residing on either the edges or motifs.

Unfortunately, all the above entropy measures usually suffer from three common theoretical drawbacks. First, these entropy measures tend to represent graph structures in the one-dimensional vectorial space from the original high-dimensional structural space. In other words, these entropy measures only provide one single characteristic value of a graph structure, leading to significant information loss. Second, most of the entropy measures mainly rely on the computation of simple structural characteristics, e.g., the information functionals for the Shannon entropy defined by Dehmer et

5

al. [23], and the vertex degree for the von Neumann entropies defined by Han and Ye et al. [29, 30]. As a result, these entropy measures can only reflect the limited and simple topological information for original graph structures. Third, most of these entropy measures can be essentially seen as the sum of the entropic features over all vertices or edges of a global graph, thus these entropy measures can only capture global graph characteristics, ignoring local graph characteristics residing on the local substructures.

To address the shortcomings of existing graph entropy measuring methods, Bai et al. [34, 35] have developed a novel framework of computing Depth-based Complexity Traces for graphs. They commence by decomposing each original graph structure into a family of k-layer expansion subgraphs rooted at a centroid vertex, and the resulting complexity trace of the original graph is defined by measuring the aforementioned Shannon entropies or the von Neumann entropies on the expansion subgraphs. Since the centroid vertex is identified by selecting the vertex that has the minimum average shortest path length to the remaining vertices, the required expansion subgraphs around the centroid vertex can provide a fine graph structure representation that gradually leads the structure from the local centroid vertex to the original global graph, as a function of structural depth. As a result, the complexity trace can not only gauge how the entropies of the expansion subgraphs vary with the increasing layer k and provide an elegant way of representing the original graph structure in a high-dimensional entropic vectorial space, but also simultaneously capture both global and local entropy-based graph characteristics. However, since the required entropy measures for the complexity trace are based on the structurally simple vertex degrees. Similar to the above graph entropy measures, the above complexity trace may not sufficiently reflect the complicated intrinsic structure information based on the simple structural features. In a summary, developing effective entropy-based graph embedding methods is always a theoretical challenging problem.

1.2. Contributions of This Work

The objective of this work is to overcome the theoretical shortcomings of the aforementioned graph entropy-based methods, by proposing a novel framework of computing Quantum-based Entropic Representations (QBER) for un-attributed graphs. One
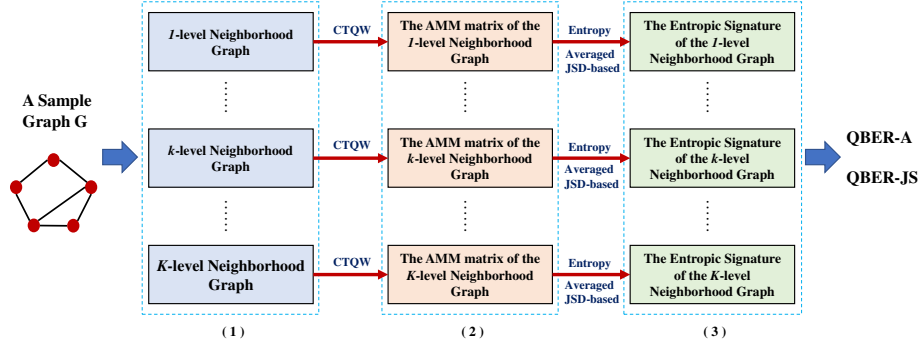
Figure 1: The proposed framework to compute the DBER of a given sample graph G. (1) Construct the family of k-level neighborhood graphs for each original graph structure, by varying the parameter k from 1 to K (i.e., the greatest value of the shortest path lengths over a set of graphs). (2) Compute the AMM matrix of the CTQW evolved on each neighborhood graph. (c) Compute the averaged and JSD-based entropic signature for each neighborhood graph, through the Quantum Shannon Entropies of the neighborhood graph vertices computed based on the AMM matrix. The resulting QBER of each original graph is computed by measuring how the entropic signatures vary on its neighborhood graphs.

key innovation of the proposed QBER approach is to compute the Quantum Shannon Entropy measures of all local vertices, through the Average Mixing Matrix (AMM) [36] of the Continuous-time Quantum Walk (CTQW) [11]. Unlike the classical random walk (e.g., the classical Steady State Random Walk (SSRW) [37]), the AMM matrix of the CTQW not only better reflects the complicated interior structure information, but also simultaneously represents both global and local structural information of the graph (see Section 2 for more details). As a result, the resulting QBER associated with the Quantum Shannon Entropies can reflect richer graph structure characteristics than existing graph entropy-based methods. The computational procedure of the proposed QBER approach is exhibited in Fig.1. Overall, the contributions of this work are summarized as follows.

First, for each graph structure, we commence by transforming the global structure into a family of neighborhood graphs, where each k-level neighborhood graph encapsulates the structural connected information between each vertex and its k-hop neighbor vertices in the original graph. We show that these neighborhood graphs can provide a fine representation of reflecting the multi-level global topological information for the

7

original graph structure.

Second, to capture complicated intrinsic structure information of the given graph, we propose to evaluate how the CTQW evolves on its family of neighborhood graphs, and employ the AMM matrix to describe the time averaged behavior of the CTQW evolved on the neighborhood graphs. The reasons of utilizing the CTQW are twofold (see more theoretical details in Section 2). First of all, it has been theoretically proven that the CTQW can better discriminate different graph structures than its classical counterpart, i.e., the classical Continuous-time Random Walk (CTRW) [38, 39]. Moreover, the AMM matrix can concisely summarize the time-averaged evolution of the CTQW, naturally providing a closest quantum analogue of the classical SSRW to compute a Shannon entropy for the graph. Specifically, we show how the AMM matrix allows us to define a Quantum Shannon Entropy for each vertex of the neighborhood graph, and thus compute an entropic signature for each neighborhood graph by measuring the averaged value or the Jensen-Shannon Divergence (JSD) [40] between the entropies of the neighborhood graph vertices. For each original graph, the resulting QBER is defined by gauging how the entropic signatures vary on its family of k-level neighborhood graphs with the increasing level k, reflecting multi-dimensional entropy-based structure information of the original graph. We show that the QBER can not only reflect complicated intrinsic structure information of the graph, but also simultaneously capture both global and local structural characteristics through the AMM matrix of the CTQW, explaining the effectiveness of the proposed QBER approach.

Third, we employ the proposed QBER approach for graph classification problems on several benchmark graph datasets, and empirically demonstrate the effectiveness of the proposed approach. The proposed approach can significantly outperform state-of-the-art entropic complexity measures, graph kernel methods, as well as graph deep learning methods.

1.3. Paper Outline

This paper is organized as follows. Section 2 introduces the concepts of the CTQW as well as its AMM matrix, and shows how to compute the Quantum Shannon Entropy associated with the AMM matrix for each vertex. Section 3 gives the theo-

retical definition of the proposed QBER approach. Section 4 empirically demonstrates the performance of the proposed QBER approach on graph classification problems. Section 5 concludes of this work.

2. Graph Entropies through the CTQW

In this section, we commence by introducing the concepts of the CTQW as well as its AMM matrix. Moreover, we show how the AMM matrix allows us to compute a Quantum Shannon Entropy for each vertex of a graph.

2.1. The AMM Matrix of the CTQW

One main objective of this paper is to employ the AMM matrix [36] of the C-TQW [11] to compute the Quantum Shannon Entropy for each graph vertex. The reason of adopting the CTQW as well as its AMM matrix is that the CTQW is theoretically different from the CTRW [41] (i.e., the classical counterpart of the CTQW) and thus has a number of interesting properties that are not available for the classical CTRW. First, the evolution of the CTQW is controlled by the time-varying unitary matrix and its state vector can be complex-valued. Thus, unlike the classical CTRW, the evolution of the CTQW is reversible, indicating that the CTQW is non-ergodic and does not possess a limited distribution. As a result, the CTQW significantly reduces the notorious tottering problem appearing in the classical CTRW. Second, the CTQW is not determined by the Laplacian spectrum associated with low frequency components, indicating that the CTQW better discriminates graph structure differences than the classical CTRW. Third, the AMM matrix can well describe the complicated evolution behavior of the CTQW, by summarizing the time-averaged vertex visiting information of the CTQW.

In this subsection, we give the concepts of the CTQW and its associated AMM matrix. Specifically, for a given graph $G(V, E)$ with the vertex set V and the edge set E, the state space of the CTQW is V. According to the Dirac notation, the basis state of the CTQW at vertex $v \in V$ is defined as $|v\rangle$, that is an orthonormal vector in a $|V|$-dimensional complex-valued Hilbert space. The state $|\psi(t)\rangle$ at time t is a complex

linear combination of the orthonormal state vectors $|v\rangle$ over all vertices $v \in V$, and is formulated as

$$|\psi(t)\rangle = \sum_{v \in V} \alpha_v(t) |v\rangle, \tag{1}$$

where $\alpha_v(t) \in \mathbb{C}$ is the complex amplitude. Unlike the classical counterpart, the evolution of the CTQW is based on the Schrödinger equation, i.e.,

$$\frac{\partial |\psi_t\rangle}{\partial t} = -i\mathcal{H} |\psi_t\rangle, \tag{2}$$

where $\mathcal{H}$ represents the system Hamiltonian and accounts for the total energy of the system, and one can adopt the adjacency matrix as the Hamiltonian.

Specifically, the behavior of the CTQW over $G(V, E)$ at time t can be described with the AMM matrix [36], i.e.,

$$
\begin{aligned}
Q_{\mathrm{M}}(t) &= U(t) \circ U(-t) \\
&= e^{i\mathcal{H}t} \circ e^{-i\mathcal{H}t},
\end{aligned} \tag{3}
$$

where the symbol $\circ$ represents the operation of the Schur-Hadamard product between $e^{i\mathcal{H}t}$ and $e^{-i\mathcal{H}t}$. Note that, since U is unitary, $Q_{\mathrm{M}}(t)$ is a doubly stochastic matrix and its entry $Q_{\mathrm{M}}(t)_{uv}$ corresponds to the probability of the CTQW visiting vertex $v \in V$ at time t when the CTQW departs from $u \in V$. To guarantee the convergence of $Q_{\mathrm{M}}(t)$, we can take the Cesàro mean and compute a time-average based AMM matrix of the CTQW as

$$Q = \lim_{T \to \infty} \int_0^T Q_M(t)dt, \tag{4}$$

where each entry Q_{vu} of the AMM matrix Q corresponds to the average probability of the CTQW visiting $u \in V$ and departing from $v \in V$, and Q is still a doubly stochastic matrix. Furthermore, since Godsil [36] has indicated that the entries of Q are rational numbers, thus one can easily compute Q from the spectrum of the Hamiltonian. Specifically, let the adjacency matrix A of G be the Hamiltonian $\mathcal{H}$, $\lambda_1, \ldots, \lambda_{|V|}$ represent the $|V|$ distinct eigenvalues of H, and P_j be the matrix representation of the orthogonal projection on the eigenspace associated with the λ_j (i.e., $\mathcal{H} = \sum_{j=1}^{|V|} \lambda_j P_j$), the AMM matrix Q of the CTQW can be rewritten as

$$Q = \sum_{j=1}^{|V|} P_j \circ P_j. \tag{5}$$

10

Remarks: Comparing to the classical random walk, the AMM matrix of the CTQW has a number of interesting properties. Specifically, Fig.2 exhibits a comparison between the AMM matrix of the CTQW and the classical Steady State Random Walk (SSRW) [37], explaining the important theoretical advantages of the CTQW. For the given graph $G(V, E)$, the probability distribution of the SSRW visiting the vertices of G is related to the vertex degree distribution [40], that is computed based on the adjacency matrix of G. Specifically, the higher degree for a vertex indicates a higher probability of the SSRW visiting the vertex. Since the degrees of the vertices v_1, v_2 and v_4 are the same (see the red and blue broken frames on the probability distribution vector of the SSRW), the probabilities of the SSRW visiting these vertices are also the same even if v_1 and v_2 have distinct structural locations with respect to v_4 in terms of the original global graph structure. In other words, the SSRW cannot discriminate the salient structural differences of the vertices through the simple use of vertex degrees. By contrast, the AMM matrix can summarize the time-averaged probability distribution of the CTQW visiting the vertices, through the complicated time evolution on the complex graph structure. Specifically, each i-th row of the AMM matrix corresponds to the probability distribution of the CTQW visiting all vertices when the CTQW departs from vertex v_i. Unlike the SSRW, the AMM matrix can provide different CTQW visiting probability distributions if the CTQW departs from the vertices having distinct structural locations. For instance, the 1-th and 2-th rows are different from the 4-row, since the vertices v_1 and v_2 are structurally different from v_4 in terms of their structural location. Moreover, each CTQW visiting probability distribution can also assign the vertices different probabilities (see the red and blue broken frames on AMM matrix). The above observations indicate that the AMM matrix not only simultaneously captures both global and local graph characteristics through the CTQW visiting probability distribution of each starting vertex, but also better reflects complicated interior graph structure information. As a result, the AMM matrix can provide us an elegant way to compute the quantum-based Shannon entropy for each vertex associated with the CTQW visiting probability distribution of the vertex, providing a multi-viewed entropy-based characteristics for a graph structure.
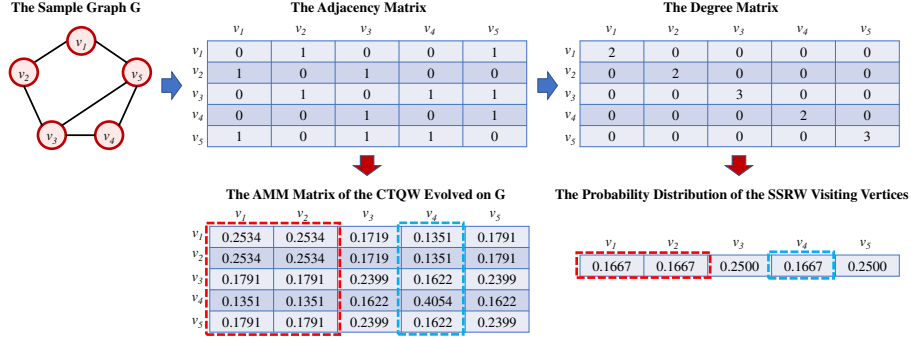
The Sample Graph G

The Adjacency Matrix

	v_1	v_2	v_3	v_4	v_5
v_1	0	1	0	0	1
v_2	1	0	1	0	0
v_3	0	1	0	1	1
v_4	0	0	1	0	1
v_5	1	0	1	1	0

The Degree Matrix

	v_1	v_2	v_3	v_4	v_5
v_1	2	0	0	0	0
v_2	0	2	0	0	0
v_3	0	0	3	0	0
v_4	0	0	0	2	0
v_5	0	0	0	0	3

The AMM Matrix of the CTQW Evolved on G

	v_1	v_2	v_3	v_4	v_5
v_1	0.2534	0.2534	0.1719	0.1351	0.1791
v_2	0.2534	0.2534	0.1719	0.1351	0.1791
v_3	0.1791	0.1791	0.2399	0.1622	0.2399
v_4	0.1351	0.1351	0.1622	0.4054	0.1622
v_5	0.1791	0.1791	0.2399	0.1622	0.2399

The Probability Distribution of the SSRW Visiting Vertices

v_1	v_2	v_3	v_4	v_5
0.1667	0.1667	0.2500	0.1667	0.2500

Figure 2: The AMM matrix of the CTQW versus the classical SSRW.

2.2. *Quantum Shannon Entropies through the CTQW*

For the given graph $G(V, E)$, since the v-th row $Q_{v,:}$ of its AMM matrix Q defined by Eq.(5) corresponds to the probability distribution of the CTQW visiting all vertices in V and departing from the vertex $v \in V$, we propose a Quantum Shannon Entropy $H_{\mathrm{QS}}(v)$ for the vertex $v \in V$ associated with Q. Specifically, $H_{\mathrm{QS}}(v)$ is formulated as

$$H_{\mathrm{QS}}(v) = H_{\mathrm{QS}}(Q_{v,:})$$
$$= -\sum_{u \in V} Q_{vu} \log Q_{vu}, \tag{6}$$

where $H_{\mathrm{QS}}(v)$ is essentially the classical Shannon entropy associated with the probability distribution $Q_{v,:}$ (i.e., the v-th row of Q). Obviously, we can compute a family of Quantum Shannon Entropies for all vertices of G.

Remarks: The proposed Quantum Shannon Entropy has two theoretical advantages. First, Fig.2 indicates that the probability distributions of the CTQW visiting all vertices are usually different, if the CTQW departs from different starting vertices that have distinct structural locations in terms of the global graph structure. Thus, for each graph, the Quantum Shannon Entropies of different vertices are usually different. This indicates that the Quantum Shannon Entropy of each vertex not only captures global structural information of the whole graph structure, but also captures the local structural characteristics of each individual vertex. In other words, the Quantum Shannon Entropy provides a way to simultaneously reflect both global and local graph structure

12

features. Second, since the CTQW can well discriminate different graph structures and reflect complicated intrinsic graph structure information. Moreover, the AMM matrix can well describe the averaged behavior of the CTQW. The Quantum Shannon Entropy associated with the AMM matrix of the CTQW can also well represent the structure information of graph structures. Overall, the Quantum Shannon Entropy provides us an elegant way to develop novel entropy-based graph embedding methods.

3. Quantum-based Entropy Representation

In this section, we propose a novel framework to compute the Quantum-based Entropic Representation (QBER) for a graph, through the AMM matrix of the CTQW evolved on the graph. We commence by introducing the concept of the JSD. Moreover, we construct a family of k-level neighborhood graphs for each original graph, and show how to compute the entropic signature of each neighborhood graph by measuring the averaged value or the JSD between the Quantum Shannon Entropies of its vertices. Finally, we give the definition of the proposed QBER approach for each graph, by gauging how the entropic signatures vary on its k-level neighborhood graphs.

3.1. The Jensen-Shannon Divergence

In information theory, the JSD is a dissimilarity measure between probability distributions [42]. For a pair of discrete probability distributions $\mathcal{X} = (x_1, \ldots, x_n, \ldots, x_N)$ and $\mathcal{Y} = (y_1, \ldots, y_n, \ldots, y_N)$, the JSD between $\mathcal{X}$ and $\mathcal{Y}$ is defined as

$$
\begin{aligned}
D_{\mathrm{JS}}(\mathcal{X}, \mathcal{Y}) &= H_{\mathrm{S}}(\frac{\mathcal{X} + \mathcal{Y}}{2}) - \frac{H_{\mathrm{S}}(\mathcal{X}) + H_{\mathrm{S}}(\mathcal{Y})}{2} \\
&= -\sum_{n=1}^{N} \frac{x_n + y_n}{2} \log \frac{x_n + y_n}{2} \\
&\quad + \sum_{n=1}^{N} x_n \log x_n + \sum_{n=1}^{N} x_n \log y_n,
\end{aligned}
\tag{7}
$$

where $H_{\mathrm{S}}(\mathcal{X}) = \sum_{n=1}^{N} x_n \log x_n$ is the classical Shannon entropy associated with the probability distribution $\mathcal{X}$.

Indeed, the JSD measure can also be employed for a mixture of M probability distributions $\mathcal{X}_1, \ldots, \mathcal{X}_i, \ldots, \mathcal{X}_I$ associated with the mixing proportions $\pi_1, \ldots, \pi_i, \ldots, \pi_I$

(i.e., $\sum_i \pi_i = 1$) , the JSD defined in Eq.(7) can be re-formulated as

$$D_{\mathrm{JS}}(\mathcal{X}_1, \ldots, \mathcal{X}_i, \ldots, \mathcal{X}_I) = H_{\mathrm{S}}(\sum_{i=1}^{I} \pi_i \mathcal{X}_i) - \sum_{i=1}^{I} \pi_i H_{\mathrm{S}}(\mathcal{X}_i). \qquad (8)$$

Note that the JSD measures D_{JS}, defined either by Eq.(7) and Eq.(8), are both well defined, symmetric, negative definite and bounded (i.e., $0 \leq D_{JS} \leq 1$). Moreover, both the JSD measures can be seen as the dissimilarities between the entropies associated with the corresponding probability distributions.

3.2. Neighborhood Graphs of Original Graph Structures

In this subsection, we show how to construct a family of k-level neighborhood graphs for each original graph $G(V, E)$. To this end, assume $\mathbf{S} \in R^{|V| \times |V|}$ denotes the shortest path matrix of the given graph $G(V, E)$, where each (v, u)-th element S_{vu} of $\mathbf{S}$ represents the shortest path between the vertices $v \in V$ and $u \in V$. The set of k-hop neighbor vertices N_v^k of the vertex $v \in V$ is defined as

$$N_v^k = \{u \in V \mid S_{vu} \leq k\}, \qquad (9)$$

i.e., N_v^k encapsulates the vertices $u \in V$ having the shortest paths of length k to the vertex $v \in V$. For the graph $G(V, E)$, the k-level neighborhood graph $G_k(V_k, E_k)$ is defined as

$$\begin{cases} \mathcal{V}_K = \{v \in V\}; \\ \mathcal{E}_K = \{(v, u) \subset N_v^k \mid S_{vu} \leq k\}. \end{cases} \qquad (10)$$

When we vary the parameter k from 1 to K (i.e., the greatest length of the shortest paths), we can construct a family of k-level neighborhood graphs as

$$\mathbf{G}_K = \{\mathcal{G}_1(\mathcal{V}_1, \mathcal{E}_1), \ldots, \mathcal{G}_k(\mathcal{V}_k, \mathcal{E}_k), \ldots, \mathcal{G}_K(\mathcal{V}_K, \mathcal{E}_K\}.$$

Since, the vertex set $\mathcal{V}_k$ of each neighborhood graph $\mathcal{G}_k$ is as same as the vertex set V of the original graph G, and the 1-level neighborhood graph $\mathcal{G}_1$ is essentially the original graph G itself, i.e., its 1-hop neighbor vertices of a vertex are essentially the adjacent vertices of the vertex. The neighborhood graphs in $\mathbf{G}_K$ can provide a fine representation of reflecting the multi-level global topological information for the original graph structure.

14

3.3. Entropic Signatures of Neighborhood Graphs

In this subsection, we show how to compute the entropic signature for each neighborhood graph through the AMM matrix of the CTQW introduced in Section 2. Specifically, for the given graph $G(V,E)$ and its associated neighborhood graph set $\mathbf{G}_K$ defined previously, we commence by performing the CTQW on each k-leve neighborhood graph $\mathcal{G}_k(\mathcal{V}_k, \mathcal{E}_k) \in \mathbf{G}_K$ and compute the associated AMM matrix $\mathcal{Q}$ based on Eq.(5). Based on Eq.(6), we propose to compute the averaged entropic signature $E_{\mathrm{A}}(\mathcal{G}_k)$ for $\mathcal{G}_k$ by calculating the averaged value between the Quantum Shannon Entropies of all vertices in $\mathcal{G}_k$ associated with $\mathcal{Q}$, i.e.,

$$
\begin{aligned}
E_{\mathrm{A}}(\mathcal{G}_k) &= \frac{1}{|\mathcal{V}_k|} \sum_{v \in \mathcal{V}_k} H_{\mathrm{QS}}(\mathcal{Q}_{v,:}) \\
&= \frac{1}{|\mathcal{V}_k|} \sum_{v \in \mathcal{V}_k} H_{\mathrm{QS}}(v) \\
&= -\frac{1}{|\mathcal{V}_k|} \sum_{v \in \mathcal{V}_k} \sum_{u \in \mathcal{V}_k} \mathcal{Q}_{vu} \log \mathcal{Q}_{vu}.
\end{aligned}
\tag{11}
$$

Moreover, based on Eq.(7), we also propose to compute the JSD-based entropic signature $E_{\mathrm{JS}}(\mathcal{G}_k)$ for $\mathcal{G}_k$ by measuring the JSD-based dissimilarity between the Quantum Shannon Entropies of all vertices in $\mathcal{G}_k$ associated with $\mathcal{Q}_k$, i.e.,

$$
\begin{aligned}
E_{\mathrm{JS}}(\mathcal{G}_k) &= D_{\mathrm{JS}}(\mathcal{Q}_{1,:}, \ldots, \mathcal{Q}_{v,:}, \ldots, \mathcal{Q}_{|\mathcal{V}_k|,:}) \\
&= H_{\mathrm{QS}}\Big(\sum_{v \in \mathcal{V}_k} \pi_v \mathcal{Q}_{v,:}\Big) - \sum_{v \in \mathcal{V}_k} \pi_v H_{\mathrm{QS}}(\mathcal{Q}_{v,:}).
\end{aligned}
\tag{12}
$$

For the above JSD measure, we propose to assign the probability distributions $\mathcal{Q}_{v,:}$ over all vertices $v \in \mathcal{V}_k$ the same proportion, i.e., $\pi_v = \frac{1}{|\mathcal{V}_k|}$. As a result, the JSD-based entropic signature $E_{\mathrm{JS}}(\mathcal{G}_k)$ defined by Eq.(12) can be re-written as

$$
\begin{aligned}
E_{\mathrm{JS}}(\mathcal{G}_k) = &-\sum_{v \in \mathcal{V}_k} \{\frac{1}{|\mathcal{V}_k|} \sum_{u \in \mathcal{V}_k} \mathcal{Q}_{vu}\} \log\{\frac{1}{|\mathcal{V}_k|} \sum_{u \in \mathcal{V}_k} \mathcal{Q}_{vu}\} \\
&+ \frac{1}{|\mathcal{V}_k|} \sum_{v \in \mathcal{V}_k} \sum_{u \in \mathcal{V}_k} \mathcal{Q}_{vu} \log \mathcal{Q}_{vu}.
\end{aligned}
\tag{13}
$$

3.4. The Definition of the QBER Approach for Graphs

In this subsection, we give the definition of the proposed Quantum-based Entropic Representation (QBER) for each original graph $G(V,E)$, through its set of neighbor-

hood graphs in $\mathbf{G}_K$. We commence by defining the QBER based on the averaged entropic signature formulated as Eq.(11).

Definition 1 (The Averaged QBER): For the given graph $G(V, E)$ and its associated k-level neighborhood graphs in $\mathbf{G}_K$, the averaged QBER $\mathrm{ER}_{\mathrm{A}}^{\mathrm{Q}}$ of G is defined as

$$\mathrm{ER}_{\mathrm{A}}^{\mathrm{Q}}(G) = [E_{\mathrm{A}}(\mathcal{G}_1), \ldots, E_{\mathrm{A}}(\mathcal{G}_k), \ldots, E_{\mathrm{A}}(\mathcal{G}_K)], \tag{14}$$

where $E_{\mathrm{A}}(\mathcal{G}_k)$ is the averaged entropic signature of the k-level neighborhood graph $\mathcal{G}_k \in \mathbf{G}_K$ of G, and the parameter k varies from 1 to K, i.e., the specified value of the greatest shortest path over all given sample graphs. ∎

Moreover, to reflect more intrinsic interior relationships between the vertices of each neighborhood graph, we also propose to define the QBER based on the JSD-based entropic signature formulated as Eq.(13), that can measure the information theoretic dissimilarity between the Quantum Shannon Entropies of the vertices.

Definition 2 (The JSD-based QBER): For the given graph $G(V, E)$ and its associated k-level neighborhood graphs in $\mathbf{G}_K$, the JSD-based QBER $\mathrm{ER}_{\mathrm{JS}}^{\mathrm{Q}}$ of G is defined as

$$\mathrm{ER}_{\mathrm{JS}}^{\mathrm{Q}}(G) = [E_{\mathrm{JS}}(\mathcal{G}_1), \ldots, E_{\mathrm{JS}}(\mathcal{G}_k), \ldots, E_{\mathrm{JS}}(\mathcal{G}_K)], \tag{15}$$

where $E_{\mathrm{JS}}(\mathcal{G}_k)$ is the JSD-based entropic signature of the k-level neighborhood graph $\mathcal{G}_k \in \mathbf{G}_K$ of G. ∎

Remarks: The above definitions indicate that both the proposed QBER approaches can represent the original graph G in a K-dimensional entropic vectorial space by gauging how the averaged or JSD-based entropic signatures of the k-level neighborhood graphs vary with the increasing parameter k. As we have stated previously, the neighborhood graphs can provide fine representations that describe multi-level global structures of the original graph, leading the structural information between 1-hop neighbor vertices (i.e., the original adjacent vertices) to that between K-hop neighbor vertices. Thus the proposed QBER approaches can reflect multi-viewed global structural characteristics in terms of the entropic signatures. Moreover, for the neighborhood graph, the Quantum Shannon Entropy of each vertex is computed through the corresponding row of the AMM matrix, that corresponds to the probability distribution of the CTQW visiting all

16

Table 1: Properties of the Proposed QBER Approaches

Theoretical Properties	QBER-A	QBER-JS	SE-SSRW [40]	SE-IF [23]	vNE [29, 30]	DBCT [34]
Capture Local Structural Information	Yes	Yes	No	No	No	Yes
Capture Global Structural Information	Yes	Yes	Yes	Yes	Yes	Yes
Reflect Intrinsic Vertex Relationship	No	Yes	No	No	No	No
Based Complicated Structure Information	Yes	Yes	No	No	No	No
Reflect Multi-dimensional Complexity	Yes	Yes	No	No	No	Yes
Computational Complexity	$O(N^3)$	$O(N^3)$	$O(N^2)$	$O(N \log N + NE)$	$O(n^2)$	$O(N \log N + NE)$

vertices when the CTQW departs from the vertex. Thus, the Quantum Shannon Entropy not only reflects the local structural information in terms of the starting vertex, but also captures the global structural information of the neighborhood graph in terms of the visiting probabilities of all vertices. As a result, the resulting QBER approaches based on the averaged value or the JSD measure between the Quantum Shannon Entropies of vertices can simultaneously capture both the global and local structure information of original graphs. Finally, as we have stated previously, the CTQW can well describe the complicated intrinsic structural information of graphs. Thus, the proposed QBER approaches through the AMM matrix of the CTQW can reflect the rich intrinsic entropic complexity information of graphs.

3.5. Discussions of Related Works

Comparing to existing state-of-the-art entropy-based graph complexity measuring methods, the proposed QBER approaches have a number of theoretical advantages, explaining the effectiveness of the proposed approaches. These properties are shown in Table 1, where QBER-A and QBER-JS correspond to the averaged QBER approach and the JS-based QBER approach defined by Eq.(14) and Eq.(15) respectively. More specifically, we briefly discuss the advantages as follows.

First, the proposed QBER approaches are defined based on the AMM matrix of the CTQW, that can not only better discriminate different graph structures but also reflect the complicated graph structure information. Moreover, the Quantum Shannon Entropies of vertices based on the AMM matrix can simultaneously encapsulate both the global and local structural information of graphs. Thus, the proposed QBER approaches can not only reflect intrinsic structural entropic complexity information, but

also simultaneously capture both global and local structural characteristics of the graph structures. By contrast, the Shannon Entropy measure based on the Information Functionals (SE-IF) [23] and that based on the State Steady Random Walk (SE-SSRW) [40], as well as the approximated von Neumann Entropy measure based on the vertex degrees (vNE) [29], can only reflect graph structural characteristics through simple graph structures or features, e.g., the information functionals of small sizes for the SE-IF entropy measure, the vertex degree distribution for the SE-SSRW entropy measure, the vertex degrees for the vNE entropy measure. Moreover, the required structures or features of these entropy measures are directly abstracted from the global graph representations of the graph structures, i.e., the vertex adjacency matrix or degree matrix. Thus, these entropy measures can only capture global characteristics of graphs. On the other hand, the proposed QBER approaches can represent the graph structures in a multi-dimensional entropic vectorial space, reflecting the multi-level entropic structure information of graphs. By contrast, the SE-IF, SE-SSRW and vNE entropy measures can only provide one-dimensional entropy-based complexity value, reflecting the limited entropy content of graphs.

Second, similar to proposed QBER approaches, the Depth-based Complexity Trace (DBCT) [34] of the graph can also represent each graph structure in a multi-dimensional entropy space, by measuring the SE-SSRW or the vNE entropy on the family of k-layer expansion subgraphs. Moreover, since the expansion subgraphs can lead the graph structure from a local centroid vertex to the global graph structure, the DBCT can also simultaneously capture both global and local structural characteristics of the graph. However, the DBCT relies on the computation of the SE-SSRW or the vNE entropy that is based on the simple graph structures or features. By contrast, the proposed QBER approaches are defined through the AMM matrix of the CTQW that can reflect complicated structure information. As a result, the proposed QBER approaches can reflect more complicated structural characteristics than the DBCT.

Third, the proposed JSD-based QBER approach is based on the JSD-based entropic signatures, that measure the JSD-based dissimilarity between the Quantum Shannon Entropies of the vertices of each neighborhood graph. In other words, the JSD-based QBER can reflect the intrinsic relationships between the vertices of each neighborhood

18

graph, capturing more complicated interior structural information residing in the depth graph structures. By contrast, the existing SE-IF, SE-SSRW and vNE entropy measures, as well as the DBCT cannot reflect any intrinsic relationship between vertices.

3.6. Computational Complexity

Computing the QBER of each graph mainly relies on two computational steps, i.e., (a) the construction of the neighborhood graphs, and (b) computing the AMM matrix of each neighborhood graph. For a graph having N vertices and M edges, the first step depends on computing the shortest path matrix of the graph, requiring the time complexity $O(N \log N + NM)$. The second step depends on the spectral decomposition, that requires the time complexity $O(N^3)$. Since M is smaller than N^2, the resulting time complexity of the proposed QBER approaches is $O(N^3)$, indicating that the proposed QBER approaches can be computed in a polynomial time.

Comparing to the computational complexity of the classical entropy-based graph complexity measuring methods discussed in Section 3.6, Table 1 shows that the proposed QBER approaches are not the most efficient algorithm in terms of the computational complexity. However, Table 1 and the discussions in Section 3.5 also indicate that the proposed QBER approaches have a number of theoretical advantages, that are not available for the classical methods. As a result, the proposed QBER approaches may have better trade-off between the classification performance and the computational efficiency, and we will empirically verify this in Section 4.

4. Experimental Evaluation

We empirically investigate the performance of the proposed QBER approaches on graph classification problems. Moreover, we compare the classification performance of the proposed QBER approaches to some state-of-the-art graph-based pattern recognition and machine learning methods, including entropy-based graph complexity measuring methods, entropy-based graph kernels, and graph deep learning methods.

19

Table 2: Statistical Information of the Benchmark Datasets.

Datasets	MUTAG	NCI1	PTC	PPIs	CATH1	CATH2	Reeb	COIL5	Shock	GatorBait
Max # vertices	28	111	109	218	568	568	220	241	33	548
Min # vertices	10	3	2	3	44	143	41	72	4	239
Mean # vertices	17.93	29.87	25.60	109.63	205.70	308.03	95.43	144.90	13.16	348.70
Max # edges	33	119	108	4493	2356	2220	219	702	32	1313
Min # edges	10	2	1	2	145	556	40	206	3	443
Mean # edges	10.79	32.30	25.96	531.50	819.85	1254.80	94.59	419	12.16	796.11
# graphs	188	4110	344	219	712	190	300	360	150	100
# classes	2	2	2	5	2	2	15	5	10	30
Description	BIO	BIO	BIO	BIO	BIO	BIO	CV	CV	CV	CV

4.1. Benchmark Dtasets

We use ten benchmark graph datasets for the experimental evaluation, and these datasets are extracted from both computer vision (CV) and bioinformatics (Bio). The Bio datasets can be found on the website [43], and the CV datasets are introduced in the references [44, 1]. More specifically, Table.2 shows the statistical details of these datasets.

4.2. Comparisons with Entropy-based Graph Complexity Measuring Methods

Experimental Setups: In this subsection, we compare the classification performance of the proposed Averaged QBER (QBER-A) and JS-based QBER (QBER-JS) approaches with some classical entropy-based graph complexity measures. These complexity measures include: (1) the Shannon Entropy based on the Information Functionals f^V (SE-FV) and f^P (SE-FP) [23], (2) the Shannon Entropy associated with the State Steady Random Walk (SE-SSRW) [40], (3) the approximated von Neumann Entropy based on the vertex degrees (vNE) [29], and (4) the Depth-based Complexity Trace [34] associated with the SE-SSRW (DBCT-SE) entropy and the vNE entropy (DBCT-vNE) respectively. For the proposed QBER-A and QBER-JS approaches on each dataset, we set the associated parameter K as the greatest value of the shortest paths over all graphs in the dataset. For the DBCT-SE and DBCT-vNE methods, we follow the same parameter setting based on the original paper. For each of the proposed

Table 3: Classification Accuracy Comparisons with Entropy-based Complexity Measures.

Datasets	MUTAG	NCI1	PTC(MR)	PPIs	CATH1
QBER-A	**84.27** $\pm$ 0.75	**73.51** $\pm$ 0.17	**58.19** $\pm$ 0.59	**76.40** $\pm$ 0.79	**98.77** $\pm$ 0.06
QBER-JS	82.97 $\pm$ 0.84	**72.33** $\pm$ 0.13	57.57 $\pm$ 0.51	**78.33** $\pm$ 0.55	**98.64** $\pm$ 0.14
SE-FV	81.04 $\pm$ 0.70	62.61 $\pm$ 0.20	56.24 $\pm$ 0.72	55.80 $\pm$ 0.87	97.86 $\pm$ 0.12
SE-FP	80.33 $\pm$ 0.71	62.50 $\pm$ 0.16	57.16 $\pm$ 0.59	56.28 $\pm$ 1.04	97.85 $\pm$ 0.11
SE-SSRW	80.91 $\pm$ 0.74	61.94 $\pm$ 0.20	55.05 $\pm$ 0.55	59.19 $\pm$ 0.80	98.31 $\pm$ 0.11
vNE	84.00 $\pm$ 0.75	62.41 $\pm$ 0.18	57.19 $\pm$ 0.59	61.04 $\pm$ 0.64	98.32 $\pm$ 0.13
DBCT-SE	81.53 $\pm$ 0.67	69.93 $\pm$ 0.13	56.67 $\pm$ 0.71	72.00 $\pm$ 0.68	98.38 $\pm$ 0.10
DBCT-vNE	82.68 $\pm$ 0.77	68.96 $\pm$ 0.10	57.97 $\pm$ 0.40	70.33 $\pm$ 0.74	98.15 $\pm$ 0.20
Datasets	CATH2	Reeb	COIL5	Shock	GatorBait
QBER-A	76.57 $\pm$ 0.91	**51.93** $\pm$ 0.66	67.27 $\pm$ 0.60	**47.88** $\pm$ 0.78	**11.10** $\pm$ 0.81
QBER-JS	**77.18** $\pm$ 0.93	**54.30** $\pm$ 0.81	67.89 $\pm$ 0.57	**44.65** $\pm$ 0.63	**10.90** $\pm$ 0.41
SE-FV	69.89 $\pm$ 0.47	27.53 $\pm$ 0.48	70.47 $\pm$ 0.58	37.06 $\pm$ 1.12	7.70 $\pm$ 0.90
SE-FP	70.78 $\pm$ 0.48	26.50 $\pm$ 0.46	69.55 $\pm$ 0.41	37.40 $\pm$ 1.21	10.80 $\pm$ 0.76
SE-SSRW	70.73 $\pm$ 0.92	25.80 $\pm$ 0.55	70.38 $\pm$ 0.71	37.00 $\pm$ 0.86	10.50 $\pm$ 0.48
vNE	71.05 $\pm$ 0.86	28.26 $\pm$ 0.80	**70.69** $\pm$ 0.57	39.06 $\pm$ 0.88	7.90 $\pm$ 0.85
DBCT-SE	76.62 $\pm$ 0.98	42.93 $\pm$ 0.62	68.04 $\pm$ 0.74	41.42 $\pm$ 1.00	5.30 $\pm$ 0.55
DBCT-vNE	75.32 $\pm$ 0.98	40.00 $\pm$ 0.63	60.88 $\pm$ 0.77	42.65 $\pm$ 0.88	5.35 $\pm$ 0.61

and alternative methods, we perform the 10-fold cross-validation strategy associated with the C-Support Vector Machine (C-SVM) [45] based on the Gaussian Kernel to compute the classification accuracy on each dataset. Specifically, we randomly divide each dataset into ten folds, and use nine folds to train the C-SVM and one fold for the test. For each method on each dataset, we employ the optimal C-SVM parameters and perform the experiment for ten times and compute the averaged classification accuracy. The experimental results (classification accuracies $\pm$ standard errors) are shown in Table 3. Moreover, we also provide the CPU runtime for each method in Table 4, that is evaluated with Matlab 2017b.

Experimental Results and Analysis: In terms of the classification accuracies, Table 3 indicates that both the proposed QBER-A and QBER-JS approaches can significantly outperform the alternative entropy-based complexity measuring methods. Specifically, the proposed approaches can achieve the best classification accuracies

Table 4: CPU Runtime Comparisons with Entropy-based Complexity Measures.

Datasets	MUTAG	NCI1	PTC(MR)	PPIs	CATH1
QBER-A	2s	3min 56s	14s	22s	18min 43s
QBER-JS	2s	4min 8s	12s	23s	19min 37s
SE-FV	1s	4s	1s	1s	10s
SE-FP	1s	4s	1s	1s	9s
SE-SSRW	1s	1s	1s	1s	1s
vNE	1s	1s	1s	1s	1s
DBCT-SE	1s	4s	1s	1s	8s
DBCT-vNE	1s	4s	1s	1s	8s
Datasets	CATH2	Reeb	COIL5	Shock	GatorBait
QBER-A	11min 29s	4min 20s	1min 30s	1s	40min 29s
QBER-JS	10min 13s	3min 46s	1min 26s	1s	41min 11s
SE-FV	1s	2s	2s	1s	5s
SE-FP	1s	2s	2s	1s	5s
SE-SSRW	1s	1s	1s	1s	1s
vNE	1s	1s	1s	1s	1s
DBCT-SE	4s	1s	2s	1s	2s
DBCT-vNE	4s	1s	2s	1s	2s

on nine of the ten datasets. For the proposed QBER-A and QBER-JS approaches, the reasons of the effectiveness are threefold. First, as we have stated previously, the alternative the SE-FV, SE-FP, SE-SSRW, vNE entropy measures can only provide the one-dimensional graph structure complexity information, and their computations mainly rely on the simple graph structure features, e.g., the information functionals and the vertex degrees. As a result, these graph entropy measures can only reflect the limited structure information of graphs. By contrast, the proposed approaches rely on measuring the averaged and JSD-based entropic signatures on a family of neighborhood graphs through the AMM matrix of the CTQW. As a result, the proposed QBER-A and QBER-JS approaches can not only provide the high-dimensional entropy-based complexity information of graphs, but also reflect more complicated interior structure information of graphs through the CTQW. Second, the SE-FV, SE-FP, SE-SSRW, vNE entropy measures can only reflect structural characteristics of global graph structures. By contrast, the proposed QBER-A and QBER-JS approaches can simultaneously reflect both global and local graph structural characteristics through the averaged and JSD-based entropic signatures, that are computed through the AMM matrix of the C-TQW. Third, on the other hand, the alternative DBCT-SE and DBCT-vNE methods can measure the entropies on a family of expansion subgraphs rooted at the centroid vertex, that leads an information content flow from the local centroid vertex to the global graph structure. Thus, similar to the proposed QBER-A and QBER-JS approaches, the alternative DBCT-SE and DBCT-vNE methods can not only provide the high-dimensional graph structure complexity information, but also simultaneously reflect both global and local structural characteristics. However, the associated entropy measures for the DBCT-SE and DBCT-vNE methods are the SE-SSRW and vNE entropy measures, that are defined based on the structurally simple vertex degrees. As a result, unlike the proposed approaches, the alternative DBCT-SE and DBCT-vNE methods cannot reflect the complicated interior graph structure information.

Furthermore, Table 3 indicates that the proposed QBER-JS approach can significantly outperform the proposed QBER-A approach on the PPIs, CATH2, Reeb, and COIL5 datasets. Furthermore, we observe that these datasets usually have more averaged vertex numbers as well as averaged edge densities (i.e., the ratio between the

23

averaged edge numbers and averaged vertex numbers) than the remaining datasets. As we defined previously, the proposed QBER-JS approach is computed by measuring the JSD-based dissimilarity (i.e., the JSD-based entropic signature) between the Quantum Shannon Entropies of the vertices for each neighborhood graph. By contrast, the proposed QBER-A approach is computed by measuring the averaged value of the Quantum Shannon Entropies. Obviously, based on the theoretical viewpoint, computing the JSD-based dissimilarity between the vertex entropies can reflect more structurally intrinsic relationships between the vertices than simply computing the averaged value of the vertex entropies. Since more averaged vertex numbers and averaged edge densities usually indicate more complicated graph structures for a graph dataset, the QBER-JS approach should have better classification performance than the proposed QBER-A approach for such a dataset, verifying that the proposed QBER-JS approach can reflect more complicated intrinsic relationship between vertices.

Finally, in terms of the CPU runtime, although the proposed QBER-A and QBER-JS approaches are not the fastest, but our approaches can still finish the computation in a meaningful polynomial time. Overall, comparing to all alternative methods, the proposed approaches have superior tradeoff between classification accuracies and computational efficiencies.

4.3. Comparisons with Graph Kernels

Experimental Setups: In this subsection, we compare the classification performance of the proposed QBER-A and QBER-JS approaches with some classical entropy-based and R-convolution graph kernel methods. These kernels include: (1) the Jensen-Shannon Graph Kernel (JSGK) [40], (2) the Jensen-Shannon Subgraph Kernel (JSSK) [46], (3) the Quantum Jensen-Shannon Graph Kernel (QJSK) [38], (4) the Entropy-based Reproducing Graph Kernel (ERGK) [47], and (5) the Graphlet Count Graph Kernel (GCGK) [48] with graphlets of size 4. Following the same experimental setup of the proposed approaches, we directly perform the 10-fold cross-validation strategy associated with the C-SVM [45] based on these alternative graph kernels. We show the averaged classification accuracy $\pm$ standard error in Table 5. Moreover, the CPU runtime for each method is exhibited in Table 4, that is evaluated with Matlab 2017b.

24

Table 5: Classification Accuracy Comparisons with Graph Kernels.

Datasets	MUTAG	NCI1	PTC(MR)	PPIs	CATH1
QBER-A	**84.27** $\pm$ 0.75	**73.51** $\pm$ 0.17	**58.19** $\pm$ 0.59	**76.40** $\pm$ 0.79	**98.77** $\pm$ 0.06
QBER-JS	82.97 $\pm$ 0.84	**72.33** $\pm$ 0.13	**57.57** $\pm$ 0.51	**78.33** $\pm$ 0.55	**98.64** $\pm$ 0.14
JSGK	83.11 $\pm$ 0.80	62.50 $\pm$ 0.33	57.29 $\pm$ 0.41	34.57 $\pm$ 0.54	98.19 $\pm$ 0.12
JSSK	83.77 $\pm$ 0.74	64.86 $\pm$ 0.24	56.94 $\pm$ 0.43	45.04 $\pm$ 0.80	98.35 $\pm$ 0.11
QJSK	82.72 $\pm$ 0.44	69.09 $\pm$ 0.20	56.70 $\pm$ 0.49	65.61 $\pm$ 0.77	98.35 $\pm$ 0.12
ERGK	84.11 $\pm$ 0.46	62.35 $\pm$ 0.13	57.52 $\pm$ 0.58	60.90 $\pm$ 0.99	98.33 $\pm$ 0.10
GCGK	82.04 $\pm$ 0.39	63.72 $\pm$ 0.12	55.41 $\pm$ 0.59	46.61 $\pm$ 0.47	97.91 $\pm$ 0.17
Datasets	CATH2	Reeb	COIL5	Shock	GatorBait
QBER-A	**76.57** $\pm$ 0.91	51.93 $\pm$ 0.66	67.27 $\pm$ 0.60	**47.88** $\pm$ 0.78	**11.10** $\pm$ 0.81
QBER-JS	**77.18** $\pm$ 0.93	**54.30** $\pm$ 0.81	67.89 $\pm$ 0.57	**44.65** $\pm$ 0.63	**10.90** $\pm$ 0.41
JSGK	72.26 $\pm$ 0.76	21.23 $\pm$ 0.76	69.13 $\pm$ 0.79	21.20 $\pm$ 0.58	7.26 $\pm$ 0.62
JSSK	75.42 $\pm$ 0.76	52.76 $\pm$ 0.47	67.75 $\pm$ 0.67	37.66 $\pm$ 0.80	9.20 $\pm$ 0.65
QJSK	71.11 $\pm$ 0.88	30.80 $\pm$ 0.61	70.11 $\pm$ 0.61	40.60 $\pm$ 0.92	9.00 $\pm$ 0.89
ERGK	70.94 $\pm$ 0.97	28.73 $\pm$ 0.37	**70.27** $\pm$ 0.69	38.20 $\pm$ 0.65	5.98 $\pm$ 0.48
GCGK	73.68 $\pm$ 1.09	22.96 $\pm$ 0.65	66.41 $\pm$ 0.63	26.93 $\pm$ 0.63	8.40 $\pm$ 0.83

Table 6: CPU Runtime Comparisons with Graph Kernels.

Datasets	MUTAG	NCI1	PTC(MR)	PPIs	CATH1
QBER-A	2s	3min 56s	14s	22s	18min 43s
QBER-JS	2s	4min 8s	12s	23s	19min 37s
JSGK	1s	6s	1s	1s	6s
JSSK	1s	52s	4s	2s	11s
QJSK	20s	2h 55min	1min 46s	3min 42s	3h 49min
ERGK	1s	5s	1s	1s	2s
GCGK	1s	5s	1s	4s	3s
Datasets	CATH2	Reeb	COIL5	Shock	GatorBait
QBER-A	11min 29s	4min 20s	1min 30s	1s	40min 29sec
QBER-JS	10min 13s	3min 46s	1min 26s	1s	41min 11sec
JSGK	1s	1s	2s	1s	1s
JSSK	4s	1s	3s	1s	3s
QJSK	1h 14min	10min 30s	18min 20s	14s	20min 53sec
ERGK	1s	1s	2s	1s	1s
GCGK	8s	2s	4s	1s	3s

Experimental Results and Analysis: In terms of the classification accuracies, Table 5 indicates that the proposed QBER-A and QBER-JS approaches can significantly outperform the alternative graph kernel methods. Specifically, the proposed approaches can achieve the best classification accuracies on nine of the ten datasets. The reasons of the effectiveness are twofold. First, the JSGK, JSSK, ERGK kernels are all defined based on the SE-SSRW and vNE entropy measures, that rely on simple graph features and only capture global graph characteristics. Thus, these kernels can only reflect the limited graph structure information in terms of the global graph structures. Moreover, the GCGK kernel is defined based on the simple graphlet substructures of small sizes. Thus, similar to the alternative entropy-based kernels, this kernel can only capture the limited local graph structure information. By contrast, the proposed QBER-A and QBER-JS approaches can not only reflect more complicated structural information through the AMM matrix of the CTQW, but also simultaneously capture both global and local graph characteristics through the associated averaged and JSD-based entropic signatures. Second, on the other hand, the alternative QJSK kernel is defined based on the CTQW. Thus, similar to the proposed approaches, the QJSK kernel can also reflect complicated graph characteristics through the CTQW. However, unlike the proposed approaches that are defined based on the AMM matrix of the CTQW, the QJSK kernel is defined by measuring the Quantum Jensen-Shannon Divergence (QJSD) between the graph density matrices of the CTQW. Since the density matrix can be seen as a structure representation of the global graph, the QJSD fails to capture local graph characteristics. By contrast, the proposed QBER-A and QBER-JS approaches can simultaneously capture both global and local graph characteristics.

Generally speaking, unlike the graph embedding methods that tend to represent the original graph structures in a low-dimensional vectorial space from the original structure space, the graph kernels can represent graph structures in a high-dimensional Hilbert space that can well preserve the graph structure information residing on the original structure space, i.e., the graph kernels usually have better performance than the graph embedding methods. However, as a kind of embedding methods, the proposed QBER-A and QBER-JS approaches can still outperform the alternative kernels, verifying the effectiveness of the proposed approaches.

26

Table 7: Classification Accuracy Comparisons with Graph Learning Methods.

Datasets	MUTAG	NCI1	PTC(MR)
QBER-A	**84.27** $\pm$ 0.75	**73.51** $\pm$ 0.17	**58.19** $\pm$ 0.59
QBER-JS	82.97 $\pm$ 0.84	72.33 $\pm$ 0.13	**57.57** $\pm$ 0.51
DCNN	66.98	56.61 $\pm$ 1.04	56.60
DGK	82.66 $\pm$ 1.45	62.48 $\pm$ 0.25	57.32 $\pm$ 1.13
DEMO-Net	81.40	−	57.20
node2vec	72.63 $\pm$ 10.20	54.89 $\pm$ 1.61	−
sub2vec	61.05 $\pm$ 15.80	52.84 $\pm$ 1.47	−
graph2vec	83.15 $\pm$ 9.25	73.22 $\pm$ 1.81	−

Finally, in terms of the CPU runtime, although the proposed QBER-A and QBER-JS approaches are not the fastest, but the computational efficiency of our approaches is still competitive to these alternative graph kernels. Considering the classification accuracies, the proposed approaches have better tradeoff between classification accuracies and computational efficiencies.

4.4. Comparisons with Graph Learning Methods

Experimental Setups: We compare the classification performance of the proposed QBER-A and QBER-JS approaches with some graph learning methods. These methods include: (1) the Deep Graph Kernel (DGK) [49], (2) the Diffusion Convolutional Neural Network (DCNN) [50], (3) the Degree Specific Graph Neural Network (DEMO-Net) [51], (4) the Scalable Feature Learning Model for Networks (node2vec) [52], (5) the Feature Learning Model for Subgraphs (sub2vec) [53], and (6) the Distributed Representation Learning Model for Graphs (graph2vec) [54]. Since these graph learning methods employ the same experimental setup with our proposed approaches, we directly report the results from the original papers in Table 7. Note that, the symbol "-" indicates that the method was not evaluated on the dataset by the original authors. Since, the original references of the alternative graph learning methods do not evaluate the CPU runtime, here we do not provide any runtime comparison.

Experimental Results and Analysis: In terms of the classification accuracies, Tabel 7 indicates that the proposed QBER-A approach can significantly outperform the

27

alternative graph learning methods on any dataset. Although, the proposed QBER-JS

approach can only achieve the best classification performance on the PTC(MR) dataset,
it is still competitive on the MUTAG and NCI1 dataset and outperforms most of the
alternative graph learning methods. Indeed, some of the alternative graph learning
methods are instances of the Graph Deep Neural Network Models, and can naturally
provide an end-to-end framework to adaptively learn meaningful graph characteristics

for classification problems. On the other hand, the proposed approaches are evaluated
by associating with the C-SVM based on the Gaussian Kernel. Essentially, this learn-
ing manner can be theoretically seen as a kind of shallow learning frameworks and
usually has lower performance than the deep learning methods. However, the proposed
approaches can still achieve the best classification performance, again indicating the

effectiveness of the proposed approaches.

5. Conclusion and Future Work

In this paper, we have developed a family of Quantum-based Entropic Representa-
tions (QBER) for un-attributed graphs, through the AMM matrix of the CTQW. Specif-
ically, the proposed QBER approaches are defined by measuring the averaged or JSD-

based entropic signatures on a family of k-level neighborhood graphs of each graph
structure. Since the neighborhood graphs can provide a fine representation to reflect
the multi-level topological information for the global structure of the original graph,
and the associated entropic signatures are computed through the AMM matrix of the
CTQW that can reflect complicated intrinsic graph structure characteristics. The pro-

posed QBER approaches not only reflect the multi-level entropic structure information
of original graphs, but also capture the complicated interior structure information re-
siding on both global and local structures. Experiments on standard graph datasets
demonstrate the effectiveness of the proposed QBER approach.

Recently, Fettal et al. [55] have proposed a multi-view graph representation learn-

ing method that not only reflects multi-view structural information like the proposed
QBER approaches, but also learns the structural characteristics for attributed graphs.
Moreover, Fang et al. [56] have developed a structure-preserving graph representation

learning method that not only captures both global and local structural characteristics like the proposed QBER approaches, but also integrates the structure learning process into the construction of graph representations. By contrast, the proposed QBER approaches are developed for un-attributed graphs, and thus cannot accommodate the edge or vertex label information. Moreover, the proposed QBER approaches rely on computing the structural characteristics through the precalculated entropic graph features in terms of the AMM matrix of the CTQW. In other words, the proposed QBER approaches cannot capture the general graph characteristics through learning the structural patterns over all graphs [57]. To address the above problems, our future work is planed to further extend the proposed QBER approaches, and develop a family of novel structure-learning based QBER approaches for attributed graphs.

Acknowledgments

References

[1] F. Escolano, E. Hancock, M. Lozano, Graph matching through entropic manifold alignment, in: CVPR, 2011, pp. 2417–2424.

[2] L. Cui, L. Bai, , X. Bai, Y. Wang, E. R. Hancock, Learning aligned vertex convolutional networks for graph classification, IEEE Trans. Neural Networks Learn. Syst. In Press (2021) 1808–1822. `doi:10.1109/TNNLS.2021.3129649.`

[3] L. Bai, Y. Jiao, L. Cui, E. R. Hancock, Learning aligned-spatial graph convolutional networks for graph classifications, in: Proceedings of ECML-PKDD, 2019, pp. 464–482.

[4] L. Bai, Y. Jiao, L. Cui, L. Rossi, Y. Wang, P. S. Yu, E. R. Hancock, Learning graph convolutional networks based on quantum vertex information propagation, IEEE Trans. Knowl. Data Eng. 35 (2) (2023) 1747–1760.

[5] J. Gasteiger, F. Becker, S. Günnemann, Gemnet: Universal directional graph neural networks for molecules, in: M. Ranzato, A. Beygelzimer, Y. N. Dauphin, P. Liang, J. W. Vaughan (Eds.), Proceedings of NeurIPS, 2021, pp. 6790–6802.

[6] L. Bai, L. Cui, Y. Jiao, L. Rossi, E. R. Hancock, Learning backtrackless aligned-spatial graph convolutional networks for graph classification, IEEE Trans. Pattern Anal. Mach. Intell. 44 (2) (2022) 783–798.

[7] K. Riesen, H. Bunke, Graph Classification and Clustering Based on Vector Space Embedding, Vol. 77 of Series in Machine Perception and Artificial Intelligence, WorldScientific, 2010.

[8] D. H. Nguyen, K. Tsuda, On a linear fused gromov-wasserstein distance for graph structured data, Pattern Recognit. 138 (2023) 109351.

[9] B. Hirchoua, S. E. Motaki, β-random walk: Collaborative sampling and weighting mechanisms based on a single parameter for node embeddings, Pattern Recognit. 142 (2023) 109730.

[10] C. T. Duong, T. T. Nguyen, T. Hoang, H. Yin, M. Weidlich, Q. V. H. Nguyen, Deep mincut: Learning node embeddings by detecting communities, Pattern Recognit. 134 (2023) 109126.

[11] D. Emms, R. C. Wilson, E. R. Hancock, Graph matching using the interference of continuous-time quantum walks, Pattern Recognition 42 (5) (2009) 985–1002.

[12] R. C. Wilson, E. R. Hancock, B. Luo, Pattern vectors from algebraic graph theory, IEEE Trans. Pattern Anal. Mach. Intell. 27 (7) (2005) 1112–1124.

[13] J. Gibert, E. Valveny, H. Bunke, Graph embedding in vector spaces by node attribute statistics, Pattern Recognition 45 (9) (2012) 3072–3083.

[14] P. Ren, R. C. Wilson, E. R. Hancock, Graph characterization via ihara coefficients, IEEE Transactions on Neural Networks 22 (2) (2011) 233–245.

[15] R. Kondor, K. M. Borgwardt, The skew spectrum of graphs, in: Proceedings of ICML, 2008, pp. 496–503.

[16] D. He, T. Wang, L. Zhai, D. Jin, L. Yang, Y. Huang, Z. Feng, P. S. Yu, Adversarial representation mechanism learning for network embedding, IEEE Trans. Knowl. Data Eng. 35 (2) (2023) 1200–1213.

[17] A. Kolmogorov, Three approaches to the definition of infornmation (in russian), Problemy Peredachi Informatsii 1 (1965) 3–11.

[18] D. Bonchev, Complexity analysis of yeast proteome network, Chemistry & biodiversity 1 (2) (2004) 312–326.

[19] D. D. Bonchev, D. Rouvray, Complexity in chemistry, biology, and ecology, Springer Science & Business Media, 2007.

[20] A. Mowshowitz, M. Dehmer, Entropy and the complexity of graphs revisited, Entropy 14 (3) (2012) 559–570.

[21] P. Pudlák, V. Rödl, P. Savickỳ, Graph complexity, Acta Informatica 25 (1988) 515–535.

[22] J. Körner, Coding of an information source having ambiguous alphabet and the entropy of graphs, in: Proceedings of Prague Conference on Information Theory, 1973, pp. 411–425.

[23] M. Dehmer, Information processing in complex networks: Graph entropy and information functionals, Applied Mathematics and Computation 201 (1-2) (2008) 82–94.

[24] M. Dehmer, A. Mowshowitz, A history of graph entropy measures, Inf. Sci. 181 (1) (2011) 57–78.

[25] M. Nielsen, I. Chuang, Quantum computation and quantum information, Cambridge university press, 2010.

[26] K. Anand, G. Bianconi, S. Severini, Shannon and von neumann entropy of random networks with heterogeneous expected degree, Physical Review E 83 (3) (2011) 036109.

[27] F. Passerini, S. Severini, Quantifying complexity in networks: the von neumann entropy, International Journal of Agent Technologies and Systems 1 (2009) 58–67.

[28] S. L. Braunstein, S. Ghosh, S. Severini, The laplacian of a graph as a density matrix: a basic combinatorial approach to separability of mixed states, arXiv preprint quant-ph/0406165.

[29] L. Han, F. Escolano, E. R. Hancock, R. C. Wilson, Graph characterizations from von neumann entropy, Pattern Recognit. Lett. 33 (15) (2012) 1958–1967.

[30] C. Ye, R. C. Wilson, C. H. Comin, L. da F. Costa, E. R. Hancock, Entropy and heterogeneity measures for directed graphs, in: Similarity-Based Pattern Recognition - Second International Workshop, SIMBAD 2013, York, UK, July 3-5, 2013. Proceedings, 2013, pp. 219–234.

[31] F. Chung, Laplacians and the cheeger inequailty for directed graphs, Annals of Combinatorics 9 (2005) 1–19.

[32] J. Wang, R. C. Wilson, E. R. Hancock, Network edge entropy decomposition with spin statistics, Pattern Recognit. 118 (2021) 108040.

[33] Z. Zhang, D. Chen, L. Bai, J. Wang, E. R. Hancock, Graph motif entropy for understanding time-evolving networks, IEEE Trans. Neural Networks Learn. Syst. 34 (4) (2023) 1651–1665.

[34] L. Bai, E. R. Hancock, Depth-based complexity traces of graphs, Pattern Recognition 47 (3) (2014) 1172–1186.

[35] L. Bai, F. Escolano, E. R. Hancock, Depth-based hypergraph complexity traces from directed line graphs, Pattern Recognit. 54 (2016) 229–240.

[36] C. Godsil, Average mixing of continuous quantum walks, Journal of Combinatorial Theory, Series A 120 (7) (2013) 1649–1662.

[37] A. Robles-Kelly, E. R. Hancock, Steady state random walks for path estimation, in: A. L. N. Fred, T. Caelli, R. P. W. Duin, A. C. Campilho, D. de Ridder (Eds.), Proceedings of S+SSPR, Vol. 3138 of Lecture Notes in Computer Science, Springer, 2004, pp. 143–152.

[38] L. Bai, L. Rossi, A. Torsello, E. R. Hancock, A quantum jensen-shannon graph kernel for unattributed graphs, Pattern Recognition 48 (2) (2015) 344–355.

[39] L. Rossi, A. Torsello, R. R. Hancock, Measuring graph similarity through continuous-time quantum walks and the quantum jensen-shannon divergence, Physical Review E 91 (2) (2015) 022815.

[40] L. Bai, E. R. Hancock, Graph kernels from the jensen-shannon divergence, Journal of Mathematical Imaging and Vision 47 (1-2) (2013) 60–69.

[41] J. Watrous, Quantum simulations of classical random walks and undirected graph connectivity, J. Comput. Syst. Sci. 62 (2) (2001) 376–391.

[42] A. F. Martins, N. A. Smith, E. P. Xing, P. M. Aguiar, M. A. Figueiredo, Nonextensive information theoretic kernels on measures, Journal of Machine Learning Research 10 (2009) 935–975.

[43] K. Kersting, N. M. Kriege, C. Morris, P. Mutzel, M. Neumann, Benchmark data sets for graph kernels (2016).
URL http://graphkernels.cs.tu-dortmund.de

[44] S. Biasotti, S. Marini, M. Mortara, G. Patanè, M. Spagnuolo, B. Falcidieno, 3d shape matching through topological structures, in: Proceedings of DGCI, 2003, pp. 194–203.

[45] C.-C. Chang, C.-J. Lin, Libsvm: A library for support vector machines, Software available at http://www.csie.ntu.edu.tw/ cjlin/libsvm.

[46] L. Bai, E. R. Hancock, Fast depth-based subgraph kernels for unattributed graphs, Pattern Recognition 50 (2016) 233–245.

[47] L. Xu, X. Jiang, L. Bai, J. Xiao, B. Luo, A hybrid reproducing graph kernel based on information entropy, Pattern Recognit. 73 (2018) 89–98.

[48] N. Shervashidze, S. Vishwanathan, T. Petri, K. Mehlhorn, K. Borgwardt, Efficient graphlet kernels for large graph comparison, Journal of Machine Learning Research 5 (2009) 488–495.

[49] P. Yanardag, S. V. N. Vishwanathan, Deep graph kernels, in: Proceedings of KDD, 2015, pp. 1365–1374.

[50] J. Atwood, D. Towsley, Diffusion-convolutional neural networks, in: Proceedings of NIPS, 2016, pp. 1993–2001.

[51] J. Wu, J. He, J. Xu, Demo-net: Degree-specific graph neural networks for node and graph classification, in: A. Teredesai, V. Kumar, Y. Li, R. Rosales, E. Terzi, G. Karypis (Eds.), Proceedings of KDD, ACM, 2019, pp. 406–415.

[52] A. Grover, J. Leskovec, node2vec: Scalable feature learning for networks, in: B. Krishnapuram, M. Shah, A. J. Smola, C. C. Aggarwal, D. Shen, R. Rastogi (Eds.), Proceedings of ACM SIGKDD, ACM, 2016, pp. 855–864.

[53] B. Adhikari, Y. Zhang, N. Ramakrishnan, B. A. Prakash, Sub2vec: Feature learning for subgraphs, in: D. Q. Phung, V. S. Tseng, G. I. Webb, B. Ho, M. Ganji, L. Rashidi (Eds.), Proceedings of PAKDD Part II, Vol. 10938 of Lecture Notes in Computer Science, Springer, 2018, pp. 170–182.

[54] A. Narayanan, M. Chandramohan, R. Venkatesan, L. Chen, Y. Liu, S. Jaiswal, graph2vec: Learning distributed representations of graphs, CoRR abs/1707.05005.

URL http://arxiv.org/abs/1707.05005

[55] C. Fettal, L. Labiod, M. Nadif, Simultaneous linear multi-view attributed graph representation learning and clustering, in: T. Chua, H. W. Lauw, L. Si, E. Terzi, P. Tsaparas (Eds.), Proceedings of ACM WSDM, ACM, 2023, pp. 303–311.

[56] R. Fang, L. Wen, Z. Kang, J. Liu, Structure-preserving graph representation learning, in: X. Zhu, S. Ranka, M. T. Thai, T. Washio, X. Wu (Eds.), Proceedings of IEEE ICDM, IEEE, 2022, pp. 927–932.

[57] D. Jin, Z. Yu, P. Jiao, S. Pan, D. He, J. Wu, P. S. Yu, W. Zhang, A survey of community detection approaches: From statistical modeling to deep learning, IEEE Trans. Knowl. Data Eng. 35 (2) (2023) 1149–1170.